Seventh International Conference on Recent Trends in Image Processing and Pattern Recognition (RTIP2R-2024)

An expert voting system for brain tumor classification using MRI images

Ha Anh Vu[a], KC Santosh[b], Szilárd Vajda[a,*]

[a]*Central Washington University, Computer Science Department, Ellensburg, WA, 98926,USA*
[b]*University of South Dakota, Computer Science Department, Vermillion, SD, 57069,USA*

Abstract

In the recent era of deep networks, the success of medical imaging has almost no limits, but the system proposed in this manuscript goes beyond imitating the expertise and decision-making of multiple radiologists. The study presents a voting system designed to enhance the accuracy of brain tumor classification through the analysis of MRI images by separate classifiers. The system uses various classifiers trained on different data representations: Support Vector Machines (SVM) and K-Nearest Neighbors (KNN) using Histogram of Oriented Gradients (HOG) features, ResNet50 using edge images (see Canny edge detector), and Convolutional Neural Networks (CNN) using the original MRI images. Each of these classifier brings unique view/decision to the ensemble, capturing different aspects of the brain scans. The voting system aggregates the predictions from these diverse models through a weighted voting mechanism, where weights are assigned based on the individual performance of each classifier. This solution balances the strengths and diminish the weaknesses of each model, leading to improved generalization and robustness. Our experimental results demonstrate that the voting system significantly outperforms the individual classifiers and other ensemble methods, achieving a remarkable accuracy rate of 98.36%. The proposed solution proves the efficacy of ensemble methods in medical image classification and demonstrates the potential of the proposed system to deliver more reliable and precise diagnostic assistance in clinical environments, thereby improving treatment strategies and patient care.

Keywords: Brain Tumor Classification; MRI Images; Voting System; Machine Learning; Ensemble Learning

1. Introduction

Classifying brain tumors through Magnetic Resonance Imaging (MRI) is essential to medical diagnostics because it impacts directly some treatment decisions and patient care. While machine learning and deep learning techniques have seen considerable advancements, accurately classifying brain tumors remains still complex due to the diverse

* Corresponding author. Tel.: +1-360-998-8999
  E-mail address: szilard.vajda@gmail.com

and intricate characteristics of tumor images, such as shape, size, texture, and variations in locations. Recent developments in Convolutional Neural Networks (CNNs) have demonstrated notable potential in analyzing medical images, particularly for detecting and categorizing brain tumors. However, individual CNN models often face limitations in generalization and robustness when applied to diverse datasets. Classical models such as Support Vector Machines (SVM) [8] or K-Nearest Neighbors (KNN) [19], also provide valuable results but typically require extensive feature manipulation and are sensitive to the quality of features.

To overcome these challenges, we propose an expert voting system that integrates several classifiers, leveraging different data representations to enhance classification accuracy and reliability. Our method leverages the combined advantages of traditional machine learning and deep learning models by utilizing Histogram of Oriented Gradients (HOG) [27] features with SVM and KNN, edge images derived from the Canny edge detector with ResNet50 [14], and original grayscale images with a custom CNN model. Extensive preliminary experiments guided us to the selection of these particular feature representations and classifiers. HOG features were particularly effective for capturing shape and texture details in SVM and KNN, while edge images improved boundary recognition in ResNet50. The CNN model extract deep hierarchical features from the grayscale image scans. This diverse set of models/features ensures a thorough analysis by capturing different aspects of the MRI data, enhancing the overall system performance.

The novelty of this manuscript is manifold): a) aggregate the predictions from a diverse set of classifiers to form a more accurate classification decision, b) the selection of the classifiers and their corresponding input is based on several metrics, including recall, precision, and F1-score, and c) the weight of each classifier is varied to find the best voting scheme. The structure of the manuscript is as follows: Section 2 provides an overview of related studies on brain tumor classification using MRI images and different machine learning techniques. Section 3 details our methodology, including data processing, feature extraction, and the configuration of the voting system. Section 4 presents our results, comparing the performance of individual models and the voting system under different scenarios. Finally, Section 5 discusses the implications of our findings and potential future work.

2. Related work

Integrating MRI scans with deep learning techniques has been widely adopted in brain tumor classification research. Traditional approaches often use single classifiers such as CNNs, transfer learning, and SVMs, alongside various image processing and segmentation techniques to enhance diagnostic accuracy [22, 2, 9]. However, challenges such as limited annotated data, high computational demands, and model interpretability remain key obstacles [21]. In this study, we propose a novel approach that employs a voting system integrating multiple classifiers [17], designed to utilize the strengths of diverse models for enhancing overall classification performance.

Several recent studies have explored ensemble learning and voting systems to improve brain tumor classification, showing similar approaches in integrating diverse models. Both Bogacsovics et al. [3] and Siar et al. [24] developed ensemble systems combining multiple CNN architectures to enhance performance. Bogacsovics et al. employed a majority voting scheme using models like AlexNet, MobileNetv2, EfficientNet, and Shufflenet v2. In contrast, Siar et al. used a weighted voting system with ResNet50, VGG-19, VGG-16, and Alexnet, assigning weights based on individual model accuracy. Despite the difference in voting strategies, both approaches emphasize the importance of model diversity and combining outputs from multiple CNNs to achieve higher classification accuracy.

Dheepak et al. [11] proposed an ensemble system comprising four customized SVM kernels (Minkowski-Gaussian, Exponential, Histogram Intersection, and Wavelet) to improve brain tumor classification. Their method integrates global and local texture features extracted using a gray-level co-occurrence matrix (GLCM) and local binary pattern (LBP), with principal component analysis (PCA) applied for dimensionality reduction.

Similarly, Munira et al. [20] proposed a model integrating different CNNs classifiers. Their system employs a voting mechanism where multiple decision trees from the Random Forest cast votes for the final classification, leading to significant improvements in multi-class brain MRI classification. The ensemble approach leverages the deep features extracted by CNNs and evaluates them through different classifiers, achieving higher accuracy than individual models.

In contrast to these approaches, our proposed method integrates machine learning and deep learning models trained on distinct data representations. We combine HOG-SVM and HOG-KNN models with edge-based ResNet50 and grayscale CNN models, utilizing a weighted voting mechanism to aggregate predictions. Each model is trained on a unique representation such as HOG features, edge images, and original grayscale MRI images. These different repre-
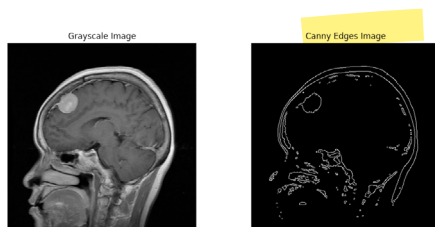
Fig. 1. Original MRI brain scan and its corresponding edge image.

sentations combined with different classifiers having completely different methodologies for creating their respective decision surfaces assure a diverse cohort of opinions, and this opinion are later combined via a weighted voting scheme.

3. Methodology

This section introduces the different data representations used for training alongside the classifiers employed in the voting system.

3.1. MRI data representations

This study utilized three different data representations of MRI images to enhance feature diversity and improve classification accuracy: HOG features, edge images derived from the Canny edge detector, and last the original grayscale images. These representations were carefully chosen to capture distinct characteristics of the images such as tumor edges or grayscale densities, thereby providing comprehensive information for the classifiers.

3.1.1. Histogram of oriented gradients

HOG [27] descriptor is a useful feature commonly employed in image processing and computer vision focusing on object detection and image recognition. It captures the gradient structure or the shape of the objects in the analyzed images, which helps identify tumors in the MRI scans.

These features were chosen because they effectively capture the edge and texture data essential for distinguishing between various categories of brain tumors. HOG descriptors are particularly useful in scenarios where the shape and structure of the object is imperative.

3.1.2. Edge images from Canny edge detector

Edge detection [5] is a popular image processing technique that helps identify boundaries. This detector was selected for its effectiveness in emphasizing the contours and boundaries of brain tumors, which are crucial for accurate classification. This method focuses on areas of rapid intensity change, typically corresponding to tumor edges. Using the Canny edge detector is particularly effective for tumor classification as it reduces the training of unnecessary pixels, thereby optimizing computational resources.

3.1.3. Grayscale Images

The original grayscale MRIs were also used to represent the data. These images retain all the original information captured by the brain scans, making them suitable for deep-learning models that can learn complex patterns using only raw pixels.

This representation was incorporated to enable deep learning models to capture and learn from the complete range of information in the MRI scans, including subtle variations in intensity and texture that might be lost in other feature extraction processes.

The images were adjusted to 256x256 pixels to minimize the data dimensionality and fit the deep network input (see CNN and ResNet50 in Section 3.2).

3.2. Classifier

This study designed and implemented a complete system for brain tumor classification using a KNN, a CNN, a ResNet50, and an SVM. Each classifier was selected for its specific strength in handling different image representations, a diverse expert system. Through rigorous preliminary experimentation with different classifiers and data representations, the highest-performing models were retained for inclusion in this research.

3.2.1. K-Nearest Neighbors

K-Nearest Neighbors (KNN) [19] is an instance-based learning strategy that classifies a new data point by relying on the majority vote of its k-nearest neighbors within the training data. It is particularly effective for datasets where local patterns can capture the data structure.

KNN was configured with $k = 3$ and applied to HOG features derived from the MRI images. The choice of $k = 3$ was made to balance sensitivity to local data structures with robustness against noise. The L2 norm was considered for the distance function due to its ability to capture the true geometric distance between data points. This norm is particularly effective for high-dimensional data like HOG features because it accounts for the magnitude and direction of differences between feature vectors, providing a more precise measure of similarity.

3.2.2. Convolutional Neural Networks (CNN-MRI)

A custom CNN model, –named CNN-MRI, was designed and developed explicitly for brain tumor classification using grayscale MRI images. The CNN-MRI model addresses the challenges of distinguishing between various brain tumor types by capturing subtle and complex visual patterns inherent in MRI scans. Unlike standard CNN architectures, CNN-MRI was optimized with a unique configuration that includes three, progressively deeper convolutional layers, each tailored to extract increasingly abstract and discriminative features.

The first layer focuses on capturing bare edges and textures, the second layer refines these features by recognizing more complex patterns, and the third layer extracts high-level, tumor-specific characteristics, such as shape and structure. This specialized design allows CNN-MRI to differentiate between similar-looking tumor classes, such as gliomas, meningiomas, and pituitary tumors. The model was configured using the Adam optimizer and the sparse categorical cross-entropy loss function, and it was trained for 60 epochs with a batch size of 32.

The CNN used in this study was trained on the original grayscale MRI images from the Figshare [6] dataset. The architecture begins with an input layer accepting images of shape (256, 256, 1). The model architecture includes three convolutional layers. The first layer employs 32 filters with a kernel size of 3×3 and ReLU activation, followed by a max-pooling layer with a pool size of 2×2. The second convolutional layer uses 64 filters with a kernel size of 3×3 and ReLU activation, accompanied by another max-pooling layer of the same size. The third layer contains some 128 filters with a 3×3 kernel size using ReLU activation and a final max-pooling layer with a pool size of 2×2.

Following the convolutional layers, the architecture incorporates a flattened layer that transforms the output of the last convolutional layer into a one-dimensional vector, preparing it for the fully connected layers. The fully connected layer consists of 128 neurons with ReLU activation and a dropout layer with a 0.5 rate to mitigate overfitting. The final output layer features several neurons corresponding to the tumor classes and applies softmax activation to categorize the input images into their respective classes.

3.2.3. ResNet50

ResNet50 [14] is a deep residual network meant to deal with the vanishing gradient problem, –enabling effective learning across layers. Its ability to capture complex features makes it ideal for tasks like medical image recognition [18, 24].

In this study, ResNet50 was deployed with pre-trained weights set up initially using the ImageNet dataset [10], which enhanced feature extraction capabilities by transferring knowledge of edges, textures, and shapes. These pre-trained weights provided a robust starting point, particularly beneficial given our limited dataset size. To adapt ResNet50 to our three-class classification task (meningioma, glioma, and pituitary tumors), the network was fine tuned by replacing the top layers with a custom classification head.

3.2.4. Support Vector Machines

Support Vector Machines (SVMs) [8] is a supervised learning strategy that excel in high-dimensional spaces by constructing a hyperplane within a multidimensional space to differentiate between the different classes.

In the experiment the SVM was trained on the HOG features. These features were chosen over the original images due to their ability to reduce the dimensionality of the data while preserving critical gradient information, which was crucial for distinguishing between different tumors. During the experiments with this classifier, we applied the seven most popular kernels, including Linear, Radial Basis Function, Polynomial, Sigmoid, Chi-Square, Laplacian, and Gaussian, to determine the model with the highest accuracy. Among these, the Linear kernel yielded the best results, and thus, it was retained for the study.
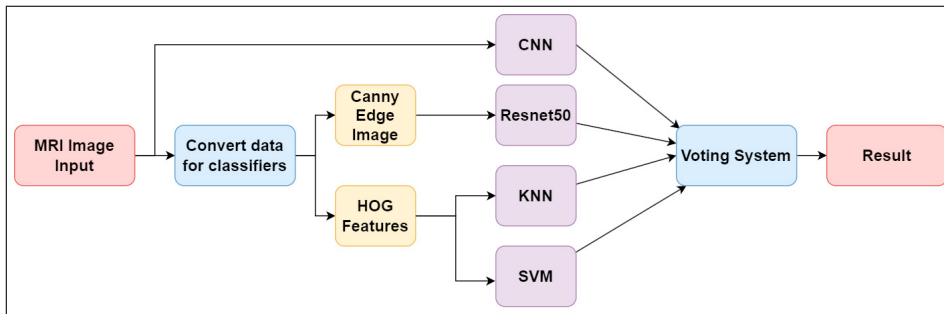
3.3. Voting System

Fig. 2. Voting system overview.

This paper introduces a comprehensive voting system that combines multiple classifiers to increase the accuracy of the individual classifiers. By exploring the strengths of both machine learning and deep learning models, the system integrates their predictions to deliver more reliable and precise results. Specifically, the approach employs classifiers such as HOG-SVM, HOG-KNN, Canny-ResNet50, and CNN, each trained on unique representations of MRI images to capture diverse feature sets crucial for robust and accurate classification.

The overall system workflow (see Fig.2) begins with loading and preprocessing the original MRI images. HOG features are extracted to capture gradient-based information vital for distinguishing tumor types. Simultaneously, original grayscale images are resized and normalized to preserve essential image details for deep learning models, while edge images from the Canny edge detector highlight the tumor boundaries. Each of these classifier processes these unique representations and makes an individual prediction.

The predictions from these classifiers are combined using a weighted voting mechanism, where each model's vote is weighted according to its accuracy. The rationale behind this approach is to ensure that the most reliable models have a greater influence on the final decision, effectively balancing the strengths of high-performing classifiers with the limitations of others. The general formula for this voting system is expressed as:

$$y_{\text{final}} = \arg\max_{c} \left(\sum_{i=1}^{n} w_i \cdot p_{i,c} \right) \tag{1}$$

where y_{final} represents the final predicted class, determined by aggregating the predictions of individual classifiers. The term c represents a particular class (see glioma, meningioma, and pituitary). The total number of classifiers used in the ensemble is denoted by n. The w_i represents the weight assigned to the i-th classifier, reflecting its accuracy or reliability. Classifiers with higher performance are given greater influence through their assigned weights. The term $p_{i,c}$ is the confidence score or probability provided by classifier i for class c. The confidence scores for each class are weighted and summed, with the class having the highest total chosen as the final prediction.
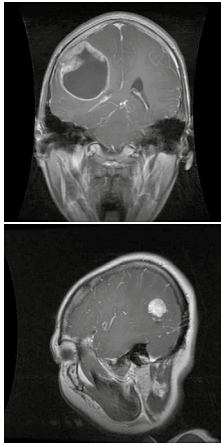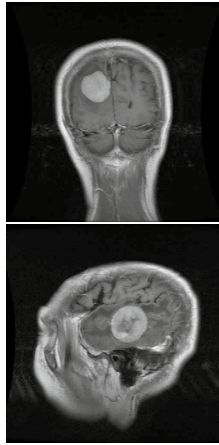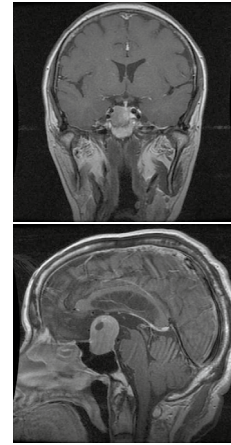
Fig. 3. Glioma samples.

Fig. 4. Meningioma samples.

Fig. 5. Pituitary samples.

4. Results

4.1. Data Description

The dataset utilized in this study [6] is a benchmark brain tumor collection and it is available on Figshare[1]. This widely recognized dataset is commonly referenced in recent brain tumor research [16, 23, 25, 18, 24]. It contains some 3064 T1-weighted MRI images, splitted into three tumors classes: glioma, meningioma and pituitary. Sample images for these tumor types are to be observed in Fig. 3, Fig. 4, and Fig. 5, respectively. One significant challenge of this dataset is the class imbalance, which mirrors real-world diagnostic conditions (see Table 1). The dataset was split into 70% for training and 30% for testing, –ensuring that the tumor categories were proportionally represented in both subsets. This division, consistent with previous studies (see Table 6), provides a fair basis for comparing our results with existing research.

Table 1. The distribution of the brain tumor dataset [6].

Class	Patient numbers	MRI slices
Meningioma	82	708
Glioma	91	1426
Pituitary	60	930
Total	**233**	**3064**

4.2. Evaluation Metrics

To benchmark the effectiveness of the proposed voting system, a multitude of metrics were considered to provide detailed insights into accuracy, precision, recall, and the model's generalization to unseen data [30, 12].

4.3. Computational Setup

Our experiments were conducted on Google Colab, utilizing the Tesla L4 GPU for handling the complexities of deep learning models and extensive datasets. We employed several key Python libraries and frameworks: TensorFlow [1] for model development, Keras [7] for a user-friendly interface, OpenCV [4] for image processing, NumPy [13] for numerical computation, and Matplotlib [15] and Seaborn [29] for data visualization .

---

[1] https://figshare.com/articles/dataset/brain_tumor_dataset/1512427

Table 2. Classification scores for KNN (HOG features).

Class	Precision	Recall	F1-Score	Support (#)
Glioma	0.93	0.99	0.96	428
Meningioma	0.98	0.85	0.91	213
Pituitary	0.99	0.97	0.99	279
Accuracy		**95.86%**		

Table 3. Classification scores for CNN-MRI (grayscale images).

Class	Precision	Recall	F1-Score	Support (#)
Glioma	0.96	0.95	0.95	428
Meningioma	0.87	0.89	0.98	213
Pituitary	0.97	0.97	0.97	279
Accuracy		**94.13%**		

Table 4. Classification scores for ResNet50 (edge images).

Class	Precision	Recall	F1-Score	Support (#)
Glioma	0.97	0.98	0.98	428
Meningioma	0.93	0.96	0.94	213
Pituitary	0.99	0.95	0.97	279
Accuracy		**96.63%**		

Table 5. Classification scores for SVM (HOG features).

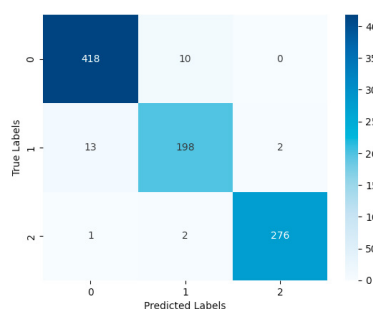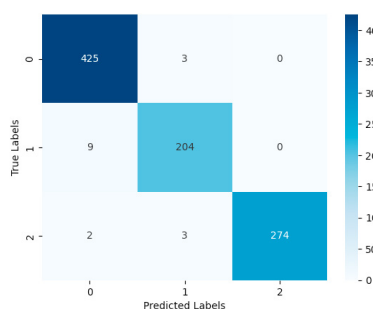| Class	Precision	Recall	F1-Score	Support (#)
Glioma	0.96	0.96	0.96	428
Meningioma	0.93	0.96	0.94	213
Pituitary	0.99	0.98	0.99	279
Accuracy		**95.54%**		

Fig. 6. Equal voting weights.

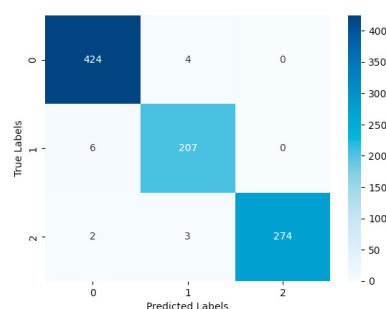Fig. 7. Incremental voting weights.

Fig. 8. Highest voting weights.

4.4. Individual Model Result

The analysis shows that each model excels in different areas of brain tumor classification (see Table 2, 3, 4, 5). ResNet50 with Canny Edge Detection achieves the highest accuracy at 96.63%, performing well for Glioma and Pituitary classes. The CNN using grayscale images follows with 94.13%, excelling in Glioma but struggling with Meningioma precision. SVM with HOG features provides balanced performance across all classes, with 95.54% accuracy. While no single model is optimal for all tumor types, a voting system enhances overall accuracy by leveraging the strengths of each model, reducing errors, and improving classification reliability.

4.5. Voting System Results

After analyzing the individual models, we combined them into a voting system and evaluated different scenarios to find the most accurate setup. The results are shown in Figs. 6, 7, and 8 . Labels 0, 1, and 2 in the previously mentioned images correspond to glioma, meningioma, and pituitary, respectively. The weights assigned are as follow: w_1 for ResNet50, w_2 for CNN-MRI, w_3 for SVM, and w_4 for KNN.

Scenario I.: All classifiers had equal weights ($w_1 = w_2 = w_3 = w_4 = 1$), leading to a 96.95% accuracy (Fig. 6). ResNet50 had the highest individual accuracy of 96.63%, but the equal weighting didn't fully exploit the classifiers' strengths.

Scenario II.: Classifiers were weighted based on performance, with the lowest receiving one vote and others incrementally more ($w_1 = 4, w_2 = 1, w_3 = 2, w_4 = 3$). This approach improved accuracy to 98.15% (Fig. 7).

Scenario III: ResNet50 was given two votes, while others received one ($w_1 = 2, w_2 = 1, w_3 = 1, w_4 = 1$). This achieved the highest accuracy of 98.36% (Fig. 8), showing the value of tailored voting weights.

Table 6. Performance comparison of the proposed framework with state-of-the-art methods on the brain tumor dataset [28].

Method	Model	Accuracy (%)	Details
Single Classifiers			
Khan et al.[16]	23-layer CNN	97.8	Train: 2454 images; Test: 610 images
Soumik et al.[25]	InceptionV3	**99.4**	5-fold cross-validation; Test: 612 images
Shnaka et al.[26]	R-CNN	94.6	Train: 2144 images; Test: 920 images
Montoya et al.[18]	ResNet50	97.3	Train: 2451 images; Test: 613 images
Vu et al. [28]	ResNet50	96.53	Train: 2144 images; Test: 920 images
Ensemble Systems			
Dheepak et al.[11]	SVM with various kernels	93.0	5-fold cross-validation; Test: 612 images
Siar et al.[24]	AlexNet, VGG-16, VGG-19, ResNet50	97.55	Train: 2450 images; Test: 614 images
Munira et al.[20]	23-layer CNN, Random Forest, SVM	96.52	Train: 2298 images; Test: 766 images
Bogacsovics et al.[3]	AlexNet, MobileNetv2, EfficientNet, ShuffleNetv2	92.0	Train: 2450 images; Test: 614 images
Proposed Method	ResNet50, KNN, SVM, CNN-MRI	**98.36**	Train: 2144 images; Test: 920 images

4.6. Alignment with state-of-the-art approaches

A detailed comparison is to be observed in Table 6, showcasing the results of various methods, including our own approach, rigorously tested and benchmarked on the same brain tumor dataset. Similar or closely aligned splits for training and testing were considered, ensuring a uniform and equitable evaluation framework for all the techniques examined.

It is to be observed that the proposed voting mechanism largely outperforms all the systems, single or ensemble alike, except the results reported in [25], which use more data to train the system, and a very computationally costly classification scheme is deployed, to achieve that result.

5. Conclusion

In this paper, we proposed a completely automatic brain tumor classification for MRI images. This approach is essential for integrating such a diagnostic system into clinical practice.

Our approach integrates multiple carefully selected classifiers, each trained on distinct data representations, including Histogram of Oriented Gradients (HOG) features, edge images from the Canny edge detector, and original grayscale images. These classifiers acts as different experts, while the features represents different viewpoints of the same brain malformation.

We aimed to create a robust and reliable diagnostic tool by leveraging the strengths of various machine learning and deep learning models, such as Support Vector Machines (SVM), K-Nearest Neighbors (KNN), ResNet50, and Convolutional Neural Networks (CNN).

The voting combines predictions from various models using weighted mechanisms, where weights reflect each model's performance. Our results show the voting system surpasses individual models and other ensemble methods, achieving up to 98.36% accuracy,notably surpassing the performance of the compared models. This underscores the effectiveness of the ensemble method in enhancing analysis and reducing misclassification.

References

[1] Abadi, M., Agarwal, A., Barham, P., Brevdo, E., Chen, Z., Citro, C., Corrado, G.S., Davis, A., Dean, J., Devin, M., Ghemawat, S., Goodfellow, I., Harp, A., Irving, G., Isard, M., Jia, Y., Jozefowicz, R., Kaiser, L., Kudlur, M., Levenberg, J., Mané, D., Monga, R., Moore, S., Murray, D., Olah, C., Schuster, M., Shlens, J., Steiner, B., Sutskever, I., Talwar, K., Tucker, P., Vanhoucke, V., Vasudevan, V., Viégas, F., Vinyals, O., Warden, P., Wattenberg, M., Wicke, M., Yu, Y., Zheng, X., 2015. TensorFlow: Large-scale machine learning on heterogeneous systems. URL: https://www.tensorflow.org/. software available from tensorflow.org.

[2] Abdusalomov, A.B., Mukhiddinov, M., Whangbo, T.K., 2023. Brain tumor detection based on deep learning approaches and magnetic resonance imaging. Cancers 15. URL: https://www.mdpi.com/2072-6694/15/16/4172, doi:10.3390/cancers15164172.

[3] Bogacsovics, G., Harangi, B., Hajdu, A., 2023. Developing diverse ensemble architectures for automatic brain tumor classification. Multimedia Tools and Applications .

[4] Bradski, G., 2000. The OpenCV Library. Dr. Dobb's Journal of Software Tools .

[5] Canny, J., 1986. A computational approach to edge detection. IEEE Transactions on Pattern Analysis and Machine Intelligence PAMI-8, 679–698. doi:10.1109/TPAMI.1986.4767851.

[6] Cheng, J., 2017. Brain tumor dataset. URL: https://doi.org/10.6084/m9.figshare.1512427.v5, doi:10.6084/m9.figshare.1512427.v5. march, 2024.

[7] Chollet, F., et al., 2015. Keras. URL: https://github.com/fchollet/keras.

[8] Cortes, C., Vapnik, V., 1995. Support-vector networks. Machine learning 20, 273–297.

[9] Cè, M., Irmici, G., Foschini, C., Danesini, G.M., Falsitta, L.V., Serio, M.L., Fontana, A., Martinenghi, C., Oliva, G., Cellina, M., 2023. Artificial intelligence in brain tumor imaging: A step toward personalized medicine. Current Oncology 30, 2673–2701. URL: https://www.mdpi.com/1718-7729/30/3/203, doi:10.3390/curroncol30030203.

[10] Deng, J., Dong, W., Socher, R., Li, L.J., Li, K., Fei-Fei, L., 2009. Imagenet: A large-scale hierarchical image database, in: 2009 IEEE Conference on Computer Vision and Pattern Recognition, pp. 248–255. doi:10.1109/CVPR.2009.5206848.

[11] Dheepak, G., Christaline, J.A., Vaishali, D., 2023. Mehw-svm multi-kernel approach for improved brain tumour classification. IET Image Processing doi:10.1049/ipr2.12345.

[12] Fawcett, T., 2006. An introduction to roc analysis. Pattern Recognition Letters 27, 861–874. URL: https://www.sciencedirect.com/science/article/pii/S016786550500303X, doi:https://doi.org/10.1016/j.patrec.2005.10.010. rOC Analysis in Pattern Recognition.

[13] Harris, C.R., Millman, K.J., van der Walt, S.J., Gommers, R., Virtanen, P., Cournapeau, D., Wieser, E., Taylor, J., Berg, S., Smith, N.J., Kern, R., Picus, M., Hoyer, S., van Kerkwijk, M.H., Brett, M., Haldane, A., del Río, J.F., Wiebe, M., Peterson, P., Gérard-Marchant, P., Sheppard, K., Reddy, T., Weckesser, W., Abbasi, H., Gohlke, C., Oliphant, T.E., 2020. Array programming with NumPy. Nature 585, 357–362. URL: https://doi.org/10.1038/s41586-020-2649-2, doi:10.1038/s41586-020-2649-2.

[14] He, K., Zhang, X., Ren, S., Sun, J., 2016. Deep residual learning for image recognition, in: 2016 IEEE Conference on Computer Vision and Pattern Recognition (CVPR), pp. 770–778. doi:10.1109/CVPR.2016.90.

[15] Hunter, J.D., 2007. Matplotlib: A 2d graphics environment. Computing in Science & Engineering 9, 90–95. doi:10.1109/MCSE.2007.55.

[16] Khan, M.S.I., et al., 2020. Accurate brain tumor detection using deep convolutional neural network. Computational and Structural Biotechnology Journal 20 (2022) .

[17] Kuncheva, L., 2007. Combining pattern classifiers: Methods and algorithms. Neural Networks, IEEE Transactions on 18, 964 – 964.

[18] Álvarez Montoya, S.F., Rojas, A.E., no Vásquez, L.F.N., 2024. Classification of brain tumors: A comparative approach of shallow and deep neural networks. SN Computer Science 5. URL: https://doi.org/10.1007/s42979-023-02431-7, doi:10.1007/s42979-023-02431-7.

[19] Mucherino, A., Papajorgji, P.J., Pardalos, P.M., 2009. k-Nearest Neighbor Classification. Springer New York, New York, NY. pp. 83–106. URL: https://doi.org/10.1007/978-0-387-88615-2_4, doi:10.1007/978-0-387-88615-2_4.

[20] Munira, H.A., Islam, M.S., 2022. Hybrid deep learning models for multi-classification of tumour from brain mri. Journal of Information Systems Engineering and Business Intelligence 8, 162–174. doi:10.20473/jisebi.8.2.162-174.

[21] Nazir, M., Shakil, S., Khurshid, K., 2021. Role of deep learning in brain tumor detection and classification (2015 to 2020): A review. Computerized Medical Imaging and Graphics 91, 101940. doi:10.1016/j.compmedimag.2021.101940.

[22] Ranjbarzadeh, R., Caputo, A., Babaee Tirkolaee, E., Ghoushchi, S., Bendechache, M., 2022. Brain tumor segmentation of mri images: A comprehensive review on the application of artificial intelligence tools. Computers in Biology and Medicine 152, 106405. doi:10.1016/j.compbiomed.2022.106405.

[23] Rasheed, Z., Ma, Y.K., Ullah, I., Ghadi, Y.Y., Khan, M.Z., Khan, M.A., Abdusalomov, A., Alqahtani, F., Shehata, A.M., 2023. Brain tumor classification from mri using image enhancement and convolutional neural network techniques. URL: https://www.mdpi.com/2076-3425/13/9/1320, doi:10.3390/brainsci13091320.

[24] Siar, M., Teshnehlab, M., 2021. A combination of feature extraction methods and deep learning for brain tumour classification. IET Image Processing 15, 1444–1456.

[25] Soumik, M.F.I., Hossain, M.A., 2020. Brain tumor classification with inception network based deep learning model using transfer learning, in: 2020 IEEE Region 10 Symposium (TENSYMP), pp. 1018–1021. doi:10.1109/TENSYMP50017.2020.9230618.

[26] Swati, Z.N.K., Zhao, Q., Kabir, M., Ali, F., Ali, Z., Ahmed, S., Lu, J., 2019. Brain tumor classification for mr images using transfer learning and fine-tuning. Computerized Medical Imaging and Graphics 75, 34–46. doi:https://doi.org/10.1016/j.compmedimag.2019.05.001.

[27] Terayama, M., Shin, J., Chang, W.D., 2009. Object detection using histogram of oriented gradients.

[28] Vu, H.A., Vajda, S., 2025. Advancing brain tumor diagnosis: A hybrid approach using edge detection and deep learning, in: Antonacopoulos, A., Chaudhuri, S., Chellappa, R., Liu, C.L., Bhattacharya, S., Pal, U. (Eds.), Pattern Recognition, Springer Nature Switzerland, Cham. pp. 226–241.

[29] Waskom, M.L., 2021. seaborn: statistical data visualization. Journal of Open Source Software 6, 3021. URL: https://doi.org/10.21105/joss.03021, doi:10.21105/joss.03021.

[30] Željko . Vujović, 2021. Classification model evaluation metrics. International Journal of Advanced Computer Science and Applications (IJACSA) 12. doi:10.14569/IJACSA.2021.0120670.